Tikrit Journal of Eng. Sciences/Vol.15/No.1/March 2008, (30-51)

NONLINEAR ANALYSIS OF CFRP- PRESTRESSED CONCRETE BEAMS SUBJECTED TO INCREMENTAL STATIC LOADING BY FINITE ELEMENTS

Dr. Husain M.Husain
Professor
Civil Eng. Dept.
University of Al- Mustansiriya

Dr. Nazar K. Oukaili
Assistant Prof.
Civil Eng. Dept.
University of Baghdad

Hakim S. Muhammed
Assistant Prof.
Technical Institute -Najaf

ABSTRACT

In this work a program is developed to carry out the nonlinear analysis (material nonlinearity) of prestressed concrete beams using tendons of carbon fiber reinforced polymer (CFRP) instead of steel. The properties of this material include high strength, light weight, and insusceptibility to corrosion and magnetism. This material is still under investigation, therefore it needs continuous work to make it beneficial in concrete design. Four beams which are tested experimentally by Yan et al. are examined by the developed computer program to reach a certain analytical approach of the design and analysis of such beams because there is no available restrictions or recommendations covering this material in the codes. The program uses the finite element analysis by dividing the beams into isoparametric 20-noded brick elements. The results obtained are good in comparison with experimental results.

KEYWORDS: FRP tendons, Prestressed concrete, Finite elements, Nonlinear materials.

INTRODUCTION

Most of prestressed concrete structures used in highway bridges and parking garages suffer from a need to continuous maintenance and rehabilitation due to steel reinforcement corrosion which is the major cause of deterioration [11]. When these structures are subjected to deicing salts or exposed to marine environment, the situation is even worse. In the last decade, research activities have surged to test and demonstrate the validity of using durable and non-corrosive materials like FRP materials to replace steel reinforcement in structures in spite of its less ductility compared to steel reinforcement [7]. There is a lack in experience and design specifications for the use of FRP materials. This paper focus on developing a computer program to be used as a nonlinear analytical approach

for the analysis of beams using FRP materials as tendons instead of steel tendons or strands. The objective is to investigate the behavior of PC (prestressed concrete) specimens and to reach to certain relations for the analysis of CFRP-prestressed concrete specimens.

MATERIAL MODELS

The materials which are used in beams fabrication are concrete and FRP tendons .The behavior of most materials under incremental static loading passes through elastic and plastic regions of failure. Because there are so many models used by engineers to investigate the behavior of these materials especially the nonlinearity property, it is very important to fix firstly the models which might be used.

Concrete Model

A plasticity-based model for the nonlinear analysis of three dimensional reinforced concrete structures under static load is adopted for the present study. The concrete model ,in compression, is simulated by an elastic –plastic work hardening model followed by a perfectly plastic response, which is terminated at the onset of crushing (Fig.(1)).

A linear elastic behavior prior to cracking is assumed, in tension model of concrete. A smeared crack model with fixed orthogonal cracks is adopted to represent the fissured concrete. The model is described in terms of cracking criterion, post- cracking criterion and shear retention models (see Figs.2&3).

Steel Model

The reinforcing bars are normally long and relatively slender, and therefore they can be generally assumed capable of transmitting axial forces only. Its stress-strain behavior can be assumed to be identical in tension and compression. In the current study ,the uniaxial stress-strain behavior of reinforcement is simulated by an elastic- linear work hardening model as shown in Fig.(4).

FRP Tendons Model

Fiber reinforced polymer tendons are referred as Strawman tendons when used in laboratory tests [6-Vol.III]. They are typically made from one of three basic fibers. These fibers are aramid ,carbon and glass .The selection of the fiber is primarily based on consideration of cost, strength, rigidity, and long term stability [6-Vol.II] .Within these fiber groups ,there are numerous different performance characteristics available

.For example , aramids may come in low, high and very high modulus configurations. Carbon fibers are also available with a large range of moduli; with upper limits four times that of steel.

There are about ten commercial types of FRP tendons as of 1997[6-Vol.I].Among these present study choose CFRP (Leadline) tendons. These tendons are developed by Mitsubishi Kasei Corporation of Japan by using a carbon FRP rods called Leadlines that are pultruded and epoxy – impregnated. The modulus of elasticity of this material is less than that of steel; therefore its durability is high. The load-strain relation used for this material is what is given by experimental tests [4 , 9] . This relationship is shown in Fig.(5) where the model used is linearly elastic up to a load of (77kN) which represents a yield stress ($f_{py} = 1488MPa$). Afterwards, the relation continues to be linear till failure where the ultimate stress is 1860MPa corresponding to a load of (96 kN).

Finite Element Formulation

In this work, the 20-node hexahedral isoparametric brick element[2] is used for idealization of concrete as shown in Fig. (6). The element has its own local coordinate system r, s, t with the origin at the center of the element such that each local coordinate ranges from (-1) to (+1).

The element stiffness matrix can be written in terms of the local coordinates (2) as follows:

$$[K]_e = \int_{-1}^{+1}\int_{-1}^{+1}\int_{-1}^{+1} [B]^T [D][B] J \, dr\,ds\,dt \quad \ldots.(1)$$

where:

$[K]_e$ = element stiffness matrix.

$[B]$ = strain-nodal displacement matrix.

$[D]$ = constitutive matrix.

$|J|$ = det. of Jacobian matrix.

Reinforced bars and prestressing tendons require a simple representation in a finite element analysis. In developing a finite element model for reinforced concrete members, at least three alternative representations of reinforcement have been used which are:

a-Distributed representation.

b-Discrete representation.

c-Embedded representation.

Among them the embedded representation is adopted in this paper

.The stiffness matrix of an embedded bar can be expressed as:

$$[K']_e = As\int_{-1}^{+1}[B]^T[D][B]h.dr \qquad \ldots\ldots\ldots\ldots(2)$$

where :

As = cross-sectional area of the bar.

$[D]$ =constitutive matrix that represents the modulus of elasticity of the steel bar.

The prestressing force is transferred to the concrete by considering the obtained stresses and strains from these forces to be an initial data read from the input of the program. These data are stored as initial stresses and strains distributed on all of the Gaussian points of the concrete and steel.

Numerical Integration

The evaluation of the element stiffness matrix involves some difficult integration. Explicit integration might be difficult or even impossible, for such functions. Usually the Gauss-Legendre scheme is used to perform the integration required to set up the element stiffness matrix .This method has been found to be accurate and convenient for finite element work[12] . In this technique the element stiffness matrix for the brick element may be written in the form:

$$[K]_e = \int_{-1}^{+1}\int_{-1}^{+1}\int_{-1}^{+1} f(r,s,t)drdsdt \cong$$

$$\sum_{i=1}^{R_1}\sum_{j=1}^{R_2}\sum_{k=1}^{R_3} W_i.W_j.W_k.f(r_i,s_j,t_k) \qquad ..(3)$$

where R_1, R_2 and R_3 are the number of Gaussian points in the r,s and t- directions respectively. The function $f(r,s,t)$ represents the matrix multiplication $([B]^T[D][B]\det[J])$. Generally the number of integration points is taken to be equal in three directions; $R_1 = R_2 = R_3 = R$.

W_i, W_j, W_k are the weight factors for i-th , j-th and k-th integration points. In a similar manner the steel bar element stiffness matrix can be written as:

$$[K']_e = \int_{-1}^{+1} f(r)dr \cong \sum_{i=1}^{R_1} W_i.f(r_i) \qquad \ldots..(4)$$

The 27(3*3*3) points of Gauss-quadrature integration rule are employed.

Non-Linear Solution Technique

The global nodal forces vector $\{f\}$ at the structural nodes are related to the nodal displacements vector $\{a\}$ by:

$$\{f\}=[K]\{a\} \qquad \ldots\ldots\ldots\ldots(5)$$

where $[K]=\sum[K]_e+[K'_e]$ is the global (structural) stiffness matrix.

Equation (5) must be solved after imposing the boundary conditions. In nonlinear problems, the stiffness matrix $[K']$ has elements depending on the unknown displacements. Therefore, methods depending on successive corrections must be used. The solution of this equation depends on obtaining balance between the external and the internal forces. To control such balance a suitable convergence tolerance must be chosen. The out of balance (residual) force vector $\{r(a)\}$ is the difference between the internal forces $\{p(a)\}$ and external forces $\{f\}$ as follows :

$$\{r(a)\}=\{p(a)\}-\{f\} \qquad \ldots\ldots\ldots\ldots(6)$$

Where, as before, $\{a\}$ represents the vector of the structural nodal displacements. The internal nodal load vector is given by:

$$\{p(a)\}=\int_{vol}[B]^T\{\sigma\}dvol \qquad \ldots\ldots.(7)$$

The solution of nonlinear problems is usually attempted by either incremental techniques, iterative techniques or a combination of them (incremental-iterative technique). In the present work, the incremental- iterative technique has been used[3 , 12] . Most nonlinear finite element problems are solved by the incremental-iterative technique. It implies the subdivision of the total external load into small proportional increments, within each increment of loading iterative cycles are performed in order to obtain a converged solution corresponding to the stage of loading under consideration Fig.(7).

The computer program developed incorporates a modified Newton-Raphson method, in which the stiffness matrix is updated at the 2nd, 12th, 22th ….etc. iterations of each increment of loading Fig. (8).

APPLICATIONS

Four beams are taken for the investigation and checking the validity of the computer program used. These beams were tested experimentally by Yan et al[11]. The configuration and geometrical shape of all the beams are shown in Fig. (9).

Due to symmetry, one quarter of the beam is taken into consideration and subdivided into 10 finite elements as shown in Fig. (10).

The beams are divided into two groups depending on their total height. Two beams are of 12 in (304mm) height and they are given B12 symbol. The other two are of 9 in (228mm) height and symboled as B9 beams. B12 and B9 beams are also subdivided into B12-4F and B12-4P and into B9-4F and B9-4Pwhich means that a beam with symbol 4F is reinforced by 4 FRP tendons fully prestressed, and the other with symbol 4P is partially prestressed reinforced by 2FRP fully prestressed and 2FRP unprestressed respectively as shown in Fig.(11).

Each selected beam quarter is divided into 10 (20-noded) isoparametric brick elements to reach a total number of nodes equal to (108) as shown in Fig.(10). The load is equally applied at nodes 30, 31, 32. More informations about material properties can be shown in Table (1).

Yan et al. make a comparison of the experimental results with two theoretical results, one based on test and the other based on model. The moment-curvature relationship of the beams being tested were analyzed based on strain compatibility and equilibrium of internal forces approach to predict their flexural response up to failure[11] .The load-deflection relationship was obtained by doubly–integrating the moment-curvature relationship with boundary conditions as for the test. Double integration of the experimental and theoretical moment-curvature curves produced theoretical load-deflection curves based on experimental results and analytical model predictions, respectively.

In the present work, the load-deflection curves from nonlinear analysis will be compared with three curves (experimental, theoretically based on test and theoretically based on model).

Results of the analysis of beam B12-4F

Fig.(13) shows the results of the present study for the load-deflection curve compared to the three curves produced by Yan et al. The results of the present analysis curve is the nearest to the experimental work compared with the other curves. It gives upper bound values of load and lower bound values of deflection throughout the behavior stages of the beam. The failure occurs when the tendon is ruptured at a failure load of 64.41 kN and deflection of 35.082 mm. The failure mode of the experimental work is exactly like that of the present study except that the failure load is 66.75 kN and deflection is 43 mm .The predicted ratio between the present and the experimental load is 0.965 which is a good ratio.

The stresses and strains in concrete over the mid-span depth are shown in Figs.(14,and 15) respectively. The compressive stresses in the upper fibers are increased as loads increased till failure occurs when the tendon is ruptured. In the early increments these stresses are tensile due to the prestressing. In the lower fibers the stresses are inverted to tension. The maximum recorded value of the compressive stress is 24.59 MPa whereas the tensile stress is 3.75 MPa.

The strains which appear in Fig. (15) are compressive strains in the upper fibers and tensile strains in the lower fibers. This phenomenon is along the ordinary behavior of the beam in all the load increments except that at the early stage where the tensile strains are in the upper fibers and the opposite (compressive strains) in the lower fibers of the concrete section. The maximum value of the compressive strain recorded is (0.00105688) in the upper fibers while in the lower fibers maximum tensile strain is (0.00562661),(with concrete being cracked).

Results of Analysis of Beam B12-4P

Beam B12-4P is reinforced by 2 CFRP Leadline prestressed tendons and 2 CFRP Leadline unprestressed tendons. The failure of this beam is due to tendon rupture in the experimental and the present work. The load-deflection curve is shown in Fig. (16). Also the present analysis curve for this beam represents the upper bound value of load and lower bound value of deflections except at the results after 50mm deflection where the load is increased by a constant value and the deflection is increased at higher rate

till failure .The values of load and deflection for the theoretical curves are representing the lower bound values except at the end region. In the same time the experimental results are representing the intermediate values between the present work and the theoretical work. The beam failed at a load of 48.02 kN and corresponding deflection of 80.62mm. The failure load in this case is less than that in case one where four prestressed tendons were used (64.41 kN), whereas the present deflection (80.62mm) is greater than that in case one (35.082mm). This means that the first beam is much stiffer due to greater number of prestressed tendons than this beam.

The distribution of normal stress on mid-span section is shown in Fig.(17) where the compressive stresses are in the upper part of the section with the maximum value (25.32MPa) and tensile stresses in the lower part with the maximum value of (4.03 MPa). The two values are greater than that in the first case (B12-4F). Due to these high stresses in compression and in tension, the corresponding strains are also high compared to the first case. The maximum recorded compressive strain is (0.00103488) while the maximum tensile strain is (0.00655591) recorded in the load increment at the ultimate load. Other strain values can be seen in Fig. (18) where there are seven curves representing the strain recorded with load increment ratios.

Results of the analysis of beam B9-4F

The difference between this beam and beam B12-4F is that the section height here is less than that of beam B12-4F. The total height of this beam is 228mm and that means the total height is decreased by 76mm which represents 25% of the section height. Number and all of the properties of CFRP tendons are kept constant Therefore this case is specified in finding the effect of decreasing height in flexural properties of CFRP beams. Fig. (19) shows the load –deflection curve of this beam compared with the experimental, theoretical based on test, and theoretical results based on model. The present analysis curve is raised from these three curves in the direction of less deflection and higher values of load. This means that the present analysis is stiff. The failure load of the present study is 37.5 kN whereas the failure load in the three

curves is 35.6 kN which means that the predicted ratio is 1.05337.

Strain distributions along mid-span depth of beam B9-4P depending on load increment ratios are shown in Fig. (21). Compressive stresses are in the upper fibers of the section and tensile stresses in the lower fibers and this is the ordinary case. In comparing these results with that of beam B12-4F, the compressive stresses are nearly approximate (close) but there is a high difference in the tensile stresses where the present case has a maximum tensile strain equal to 0.00348889 while that for case B12-4F equal to 0.00562661 and that is because of decreasing the total height of the beam B9-4F.

Results of the analysis of beam B9-4P

The difference between this beam and the previous beam B9-4F is that two of the four tendons are unprestressed and they are in the lower layer. This case is examined here to see the effect of this variation. The output results are shown in Fig.(22) .It is clear from the graph that the early results up to about 20% of the total load are nearly coinciding and that is expectable because the behavior is within the elastic range. Afterwards, as is load increased the recorded deflection is less than that predicted for the other curves up to 90% of the total load where the deflection is 120mm while in the other three curves are 120,140 and 165mm respectively.

The total failure load in this case is less than in all other cases because the strength capacity of the section is decreased in two ways, height reduction and unprestressing of two tendons.

The results of stresses and strains along mid-span depth are shown in Figs.(23,and 24) respectively. The values of stresses in this case are approximately equal with the values of the previous beam B9-4F except that at increment ratio 90% there is a clear difference between the two. The maximum compressive force in the upper fibers of this case at load increment 100% (ultimate load) is 23.6 MPa while that in case B9-4F is 22.67 MPa. The corresponding strains of the present case appear in Fig. (24) where compressive strains in the upper fibers appear and tensile stresses are in the lower fibers. The maximum tensile strain is 0.00101452 which is recorded at an increment of 100% ratio (ultimate load) and at Gaussian point number 32. It can be seen that due to rising of prestressing

force in the lower two tendons, the maximum compressive and tensile stresses are increased.

CONCLUSIONS AND RECOMMENDATIONS

Based on the results of using this developed program for the analysis of CFRP-prestressed concrete beams the following conclusions are drawn:

1. The behavior of FRP beams is affected by parameters such as reinforcement ratio, cross-section dimensions, and prestressing pattern.

2. The use of the developed program gave close results with experimental work where the predicted ratio recorded between the present and the experimental load is not less than 0.949.

3. The present analysis curves for all beams tested show stiff behavior which means that this material (FRP) needs more ductility compared to steel reinforcement.

4. A parametric study in the present work is not carried out but it was done in the experimental work of Yan et al. and according to their conclusions it can be concluded in the present study that decreasing the total height by 25% will decrease the failure load by about 41% for the example considered.

The following recommendations can be drawn:

1. More experimental study must be done to improve ductility properties of this new material.

2. Many recommendations were mentioned in the final report of the three groups of Wyoming, Pennsylvania, and Missouri-Rolla Universities, but more study is needed to give high confidence in using this material.

3. More theoretical work is also needed to reach final expressions for the design and analysis of structures containing this material.

4. The validity of the developed program can be tested when using composite structures like:

a. steel girder with FRP-reinforced or prestressed slabs.

b. prestressed concrete girders with FRP tendons and cast-in- place slabs.

c. prestressed concrete girders with FRP tendons and prestressed cast-in-place slabs

REFERENCES

1. Al-Shaarbaf I.A.S., "Three-dimensional non-linear finite element analysis of reinforced concrete beams in torsion", PhD. Thesis, University of Bradford, 1990.

2. Bathe K.J., "Finite Element Procedures", Prentice-Hall, Inc., New Jersey, 1996.

3. Bathe K.J. and Ramaswamy S., "On three- dimensional nonlinear analysis of concrete structures", Nuclear Engineering and Design, Vol.52, 1979.

4. Castro P.F. and Carino N.J., "Tensile and nondestructive testing of FRP bars". J. of composites and construction,Feb.1998.

5. Chen W.F., "Plasticity in reinforced concrete", McGraw-Hill Book Co., Third Edition, London, 1982.

6. "Design and recommendations for concrete structures prestressed with FRP tendons", FHWA contract, DTFH61-96-C-00019, Final report August, 2001. Prepared by Dolan C.W. & Hamilton H.R. (Wyoming University), Bakis C.E. (Pennsylvania State University), and Nanni A. (University of Missouri-Rolla). Volumes I , II , and III .

7. Harris H.G., Somboonson W., and Ko F.K. "New ductile hybrid FRP reinforcing bar for concrete structures", J. of Composites and Construction, Feb.1998.

8. Khachaturian N. and Gurfinkel G., "Prestressed concrete", McGraw-Hill Book Co., USA, 1969.

9. Rostasy F.S. "Draft guidelines for the acceptance testing of FRP posttensioning tendons". J. of composites and construction, Feb.1998.

10. State-of-the-Art Report on "Finite element analysis of reinforced concrete", ASCE, 1982.

11. Yan X. ,Myers J.J. and Nanni A. "An assessment of flexural behavior of CFRP prestressed beams subjected to incremental static loading" .,ASCE Structures Congress 2000,Philadelphia ,PA,(2000).

12. Zienkiewicz O.C ,"The finite element method", McGraw-Hill Book Co., Third edition, London 1977.

Table (1): Properties of the materials used in fabrication of beams

Material / Beam used	B12-4F	B12-4P	B9-4F	B9-4P
Concrete				
Compressive strength f_c' (MPa)	41.72	55.167	41.72	55.167
Modulus of elasticity E_C^* (MPa)	30000	34900	30000	34900
Tensile strength f_t^{**} (MPa)	4.5	5.2	5.2	4.5
Poisson's ratio υ	0.2	0.2	0.2	0.2
Steel Reinforcement				
Elastic modulus E_S (MPa)	200000	200000	200000	200000
Yield stress f_y (MPa)	410	410	410	410
Area of steel A_S (mm^2)	------	-------	-------	-------
CFRP Prestressed Tendons				
Elastic modulus E_p (MPa)	153345	153345	153345	153345
Yield stress f_{py} (MPa)	1488	1488	1488	1488
Initial prestress f_{pi} (MPa)	1116	1116	1116	1116
Initial prestressing force P_i (kN)	231	115.5	231	115.5
Number of prestressed FRP tendons	4	2	4	2
Area of prestressed FRP tendons(mm^2)	207	103.5	207	103.5
Number of unprestressed FRP tendons	----------	2	---------	2
Area of unprestressed FRP tendons(mm^2)	----------	100.6	---------	100.6

* $E_c = 4700\sqrt{f_c'}$ -(ACI-Building Code 318 M-02)

** $f_t = 0.7\sqrt{f_c'}$ -(ACI-Building Code 318 M-02)

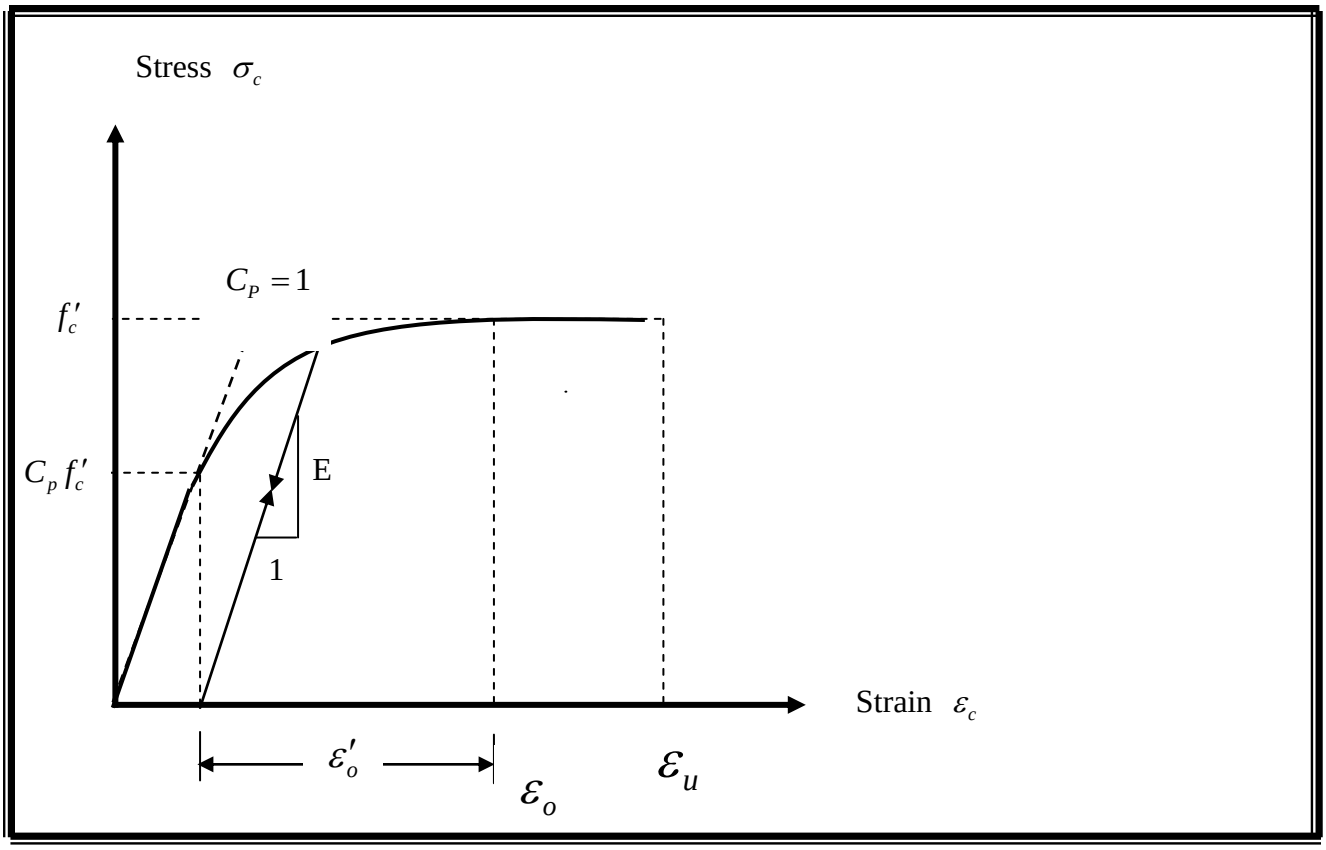

Fig.(1) Uniaxial stress –strain curve of concrete in compression (5)

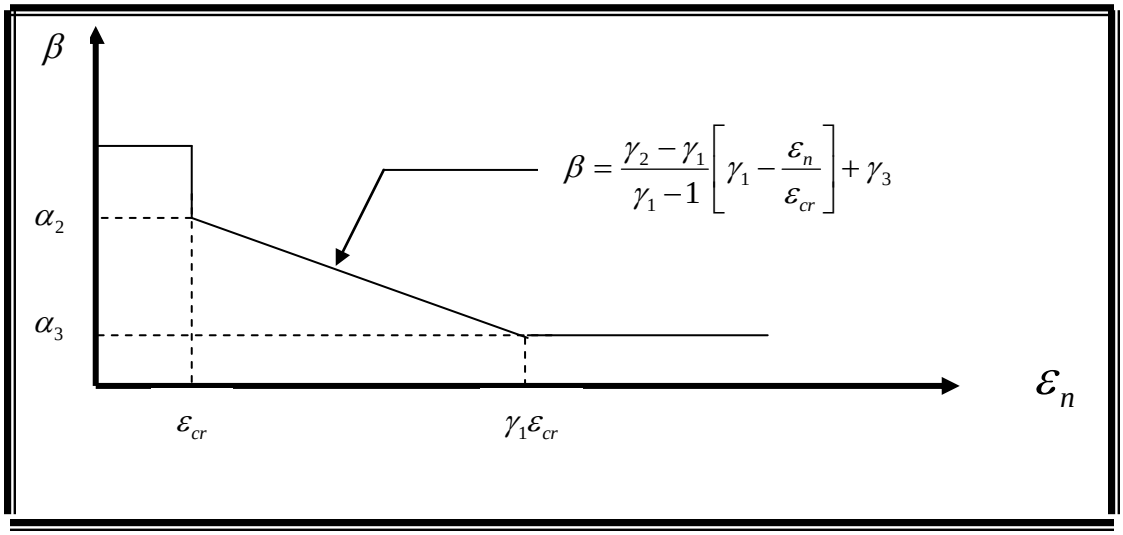

Fig.(2) Post-cracking model for concrete in tension (1)

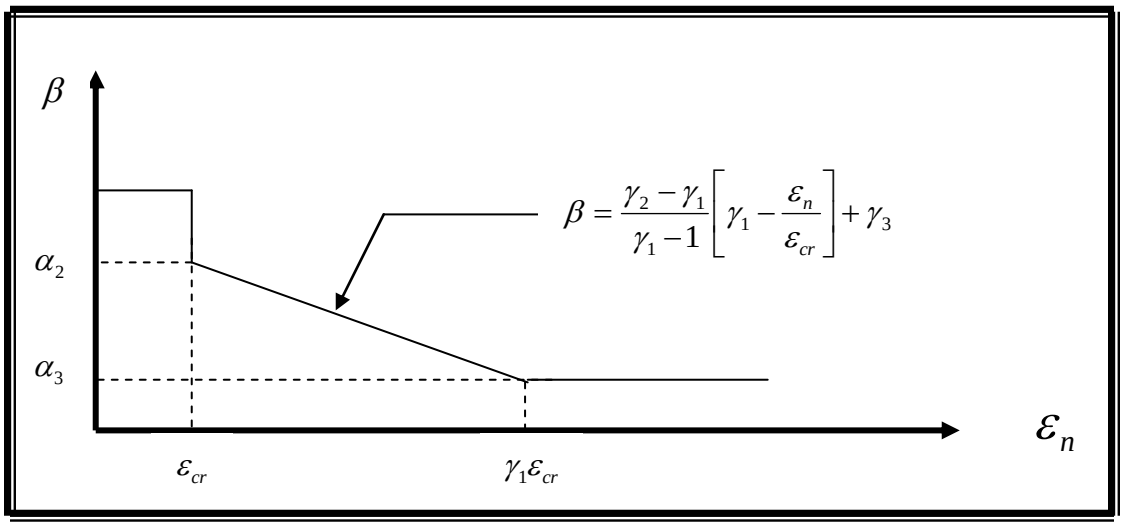

Fig.(3) Shear retention model for concrete (1)

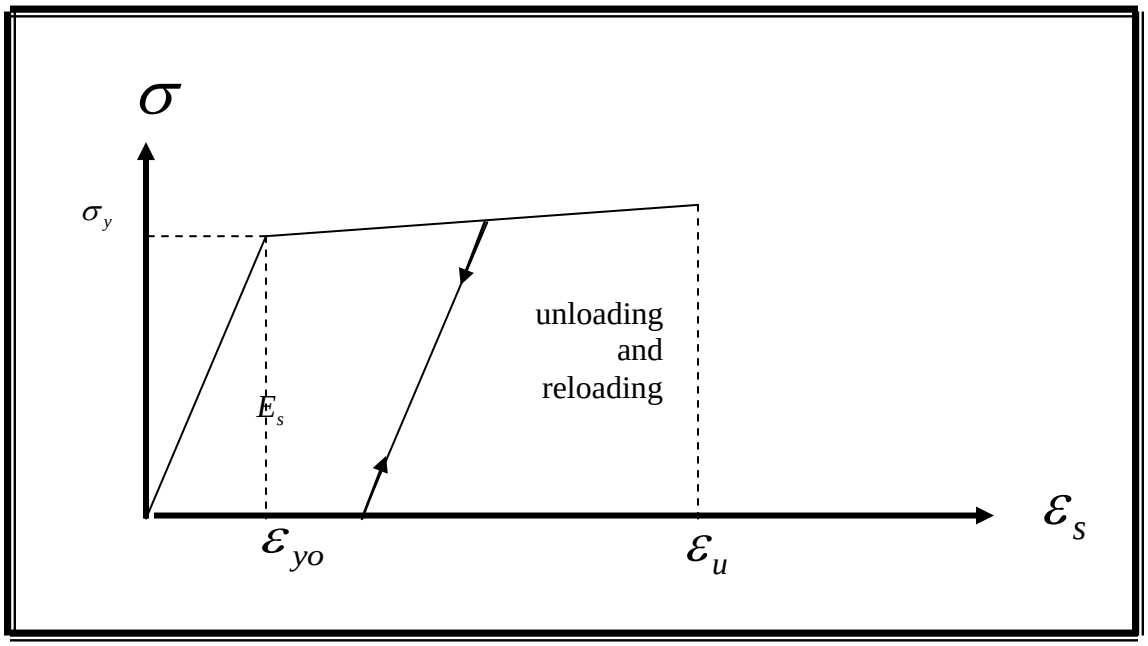

Fig.(4) Stress-strain relationship of steel bars used in the analysis [8,10]

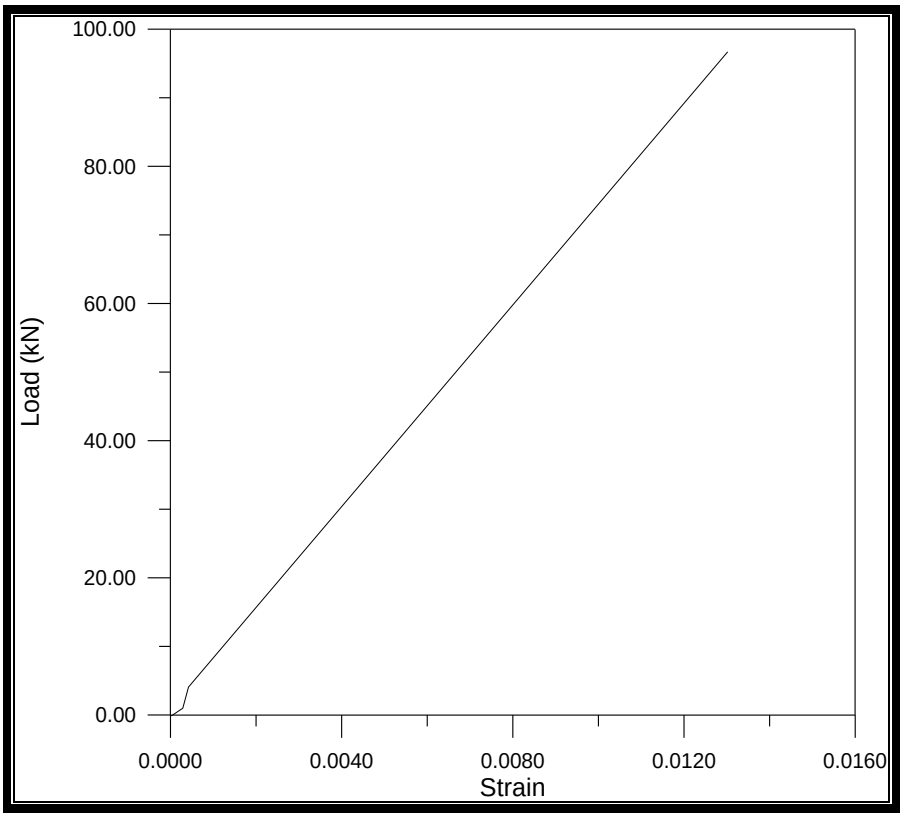

Fig.(5) Typical load-strain curve for the Strawman tendons [6]

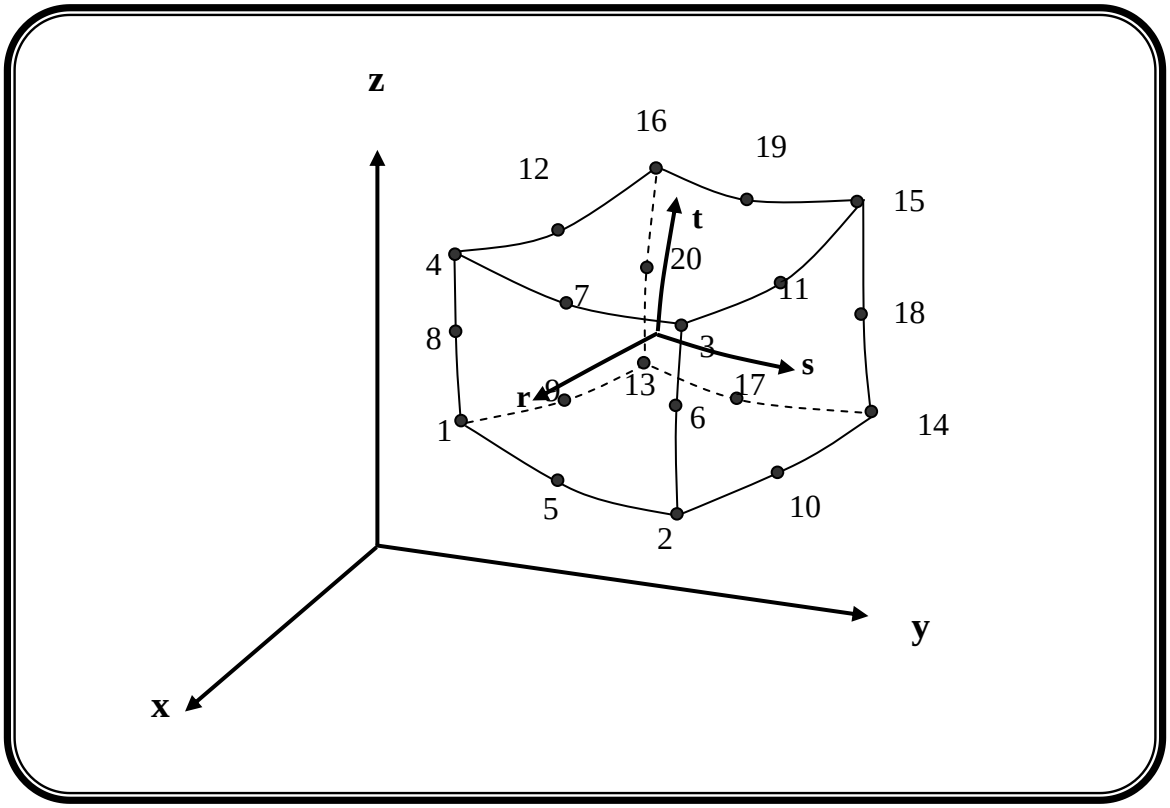

Fig.(6): The 20-node brick element in Cartesian coordinates[2]

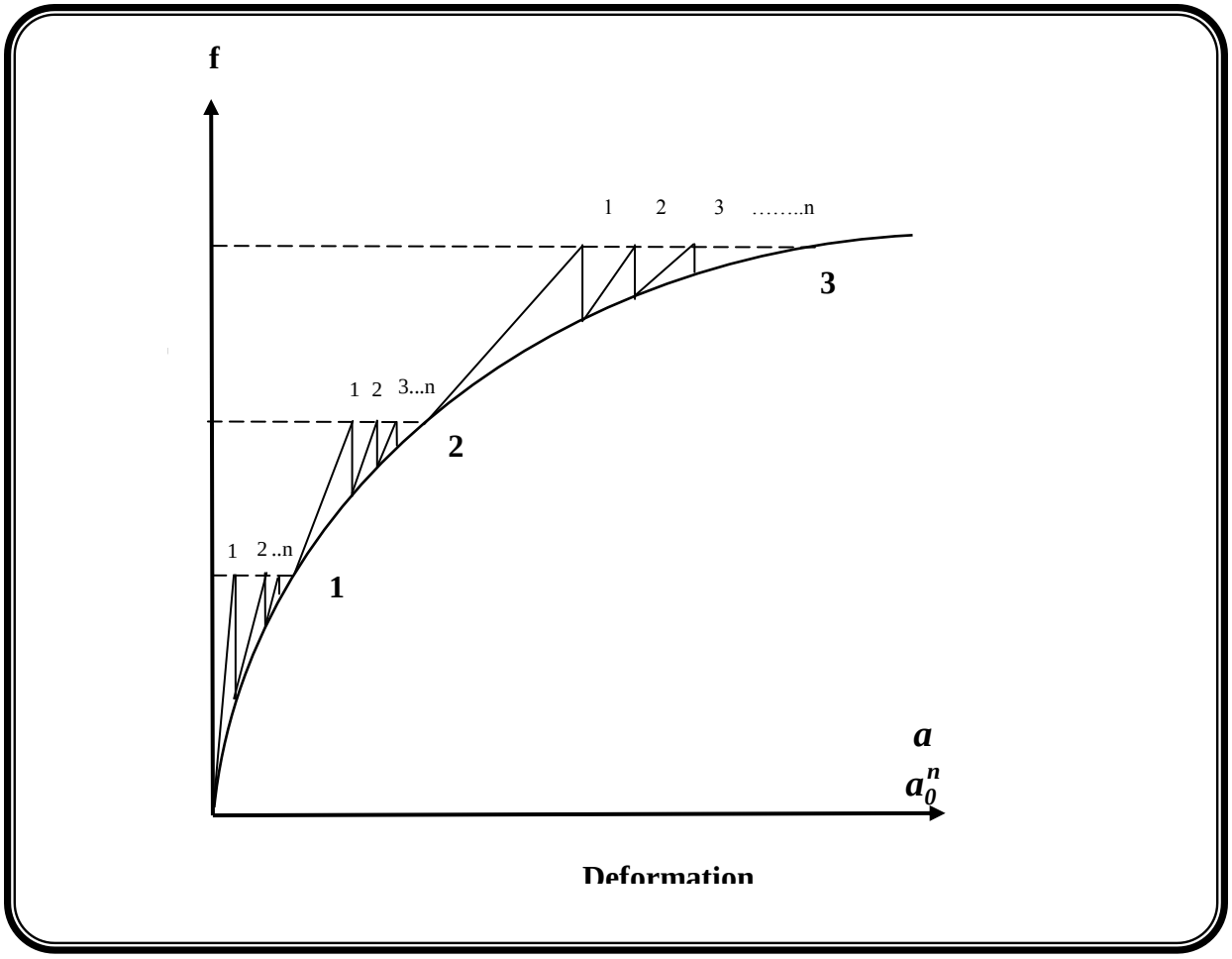

Fig.(7): Incremental- Iterative technique

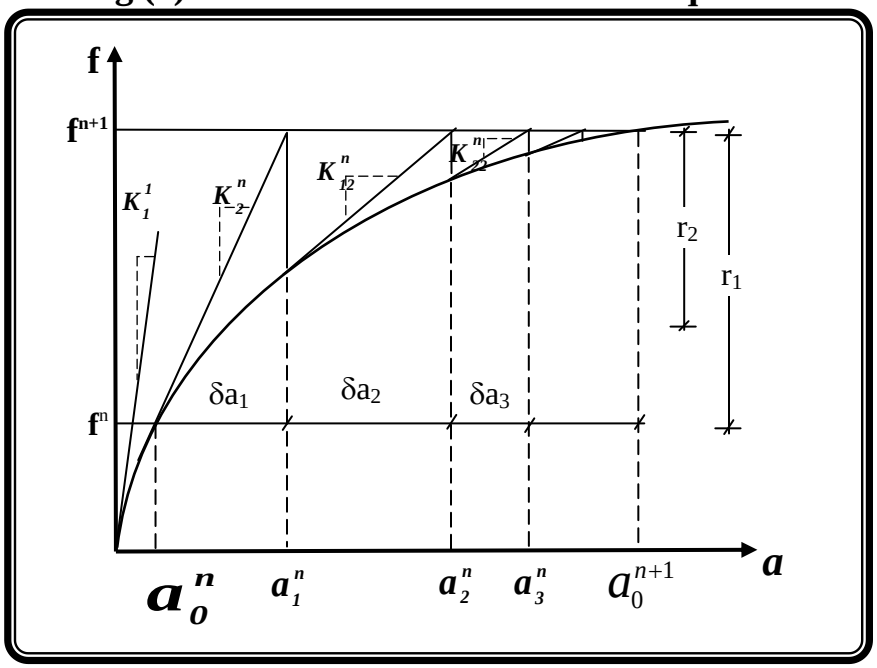

Fig.(8): Modified Newton –Raphson method.

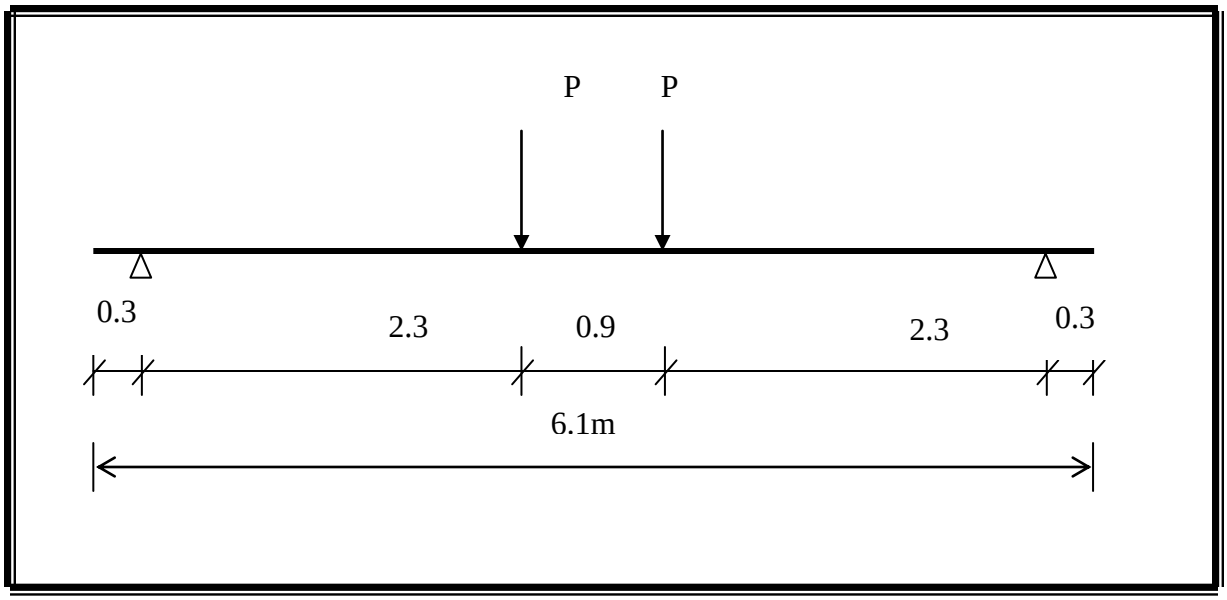

Fig.(9): Dimensions of the beams tested by Yan et al.

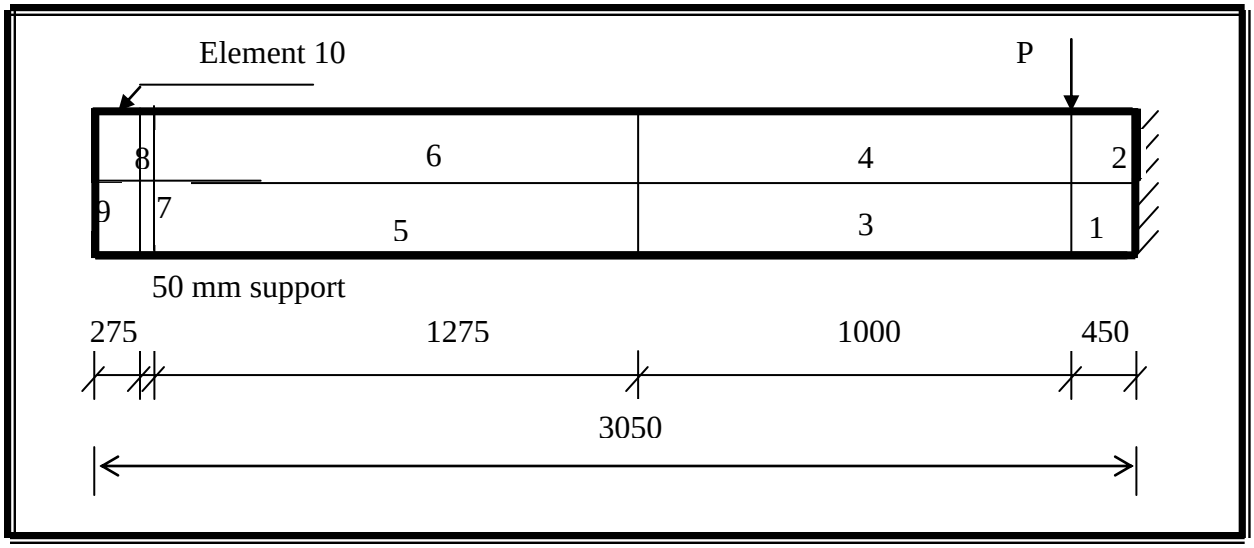

Fig. (10): The selected quarter of the beam and the mesh of elements

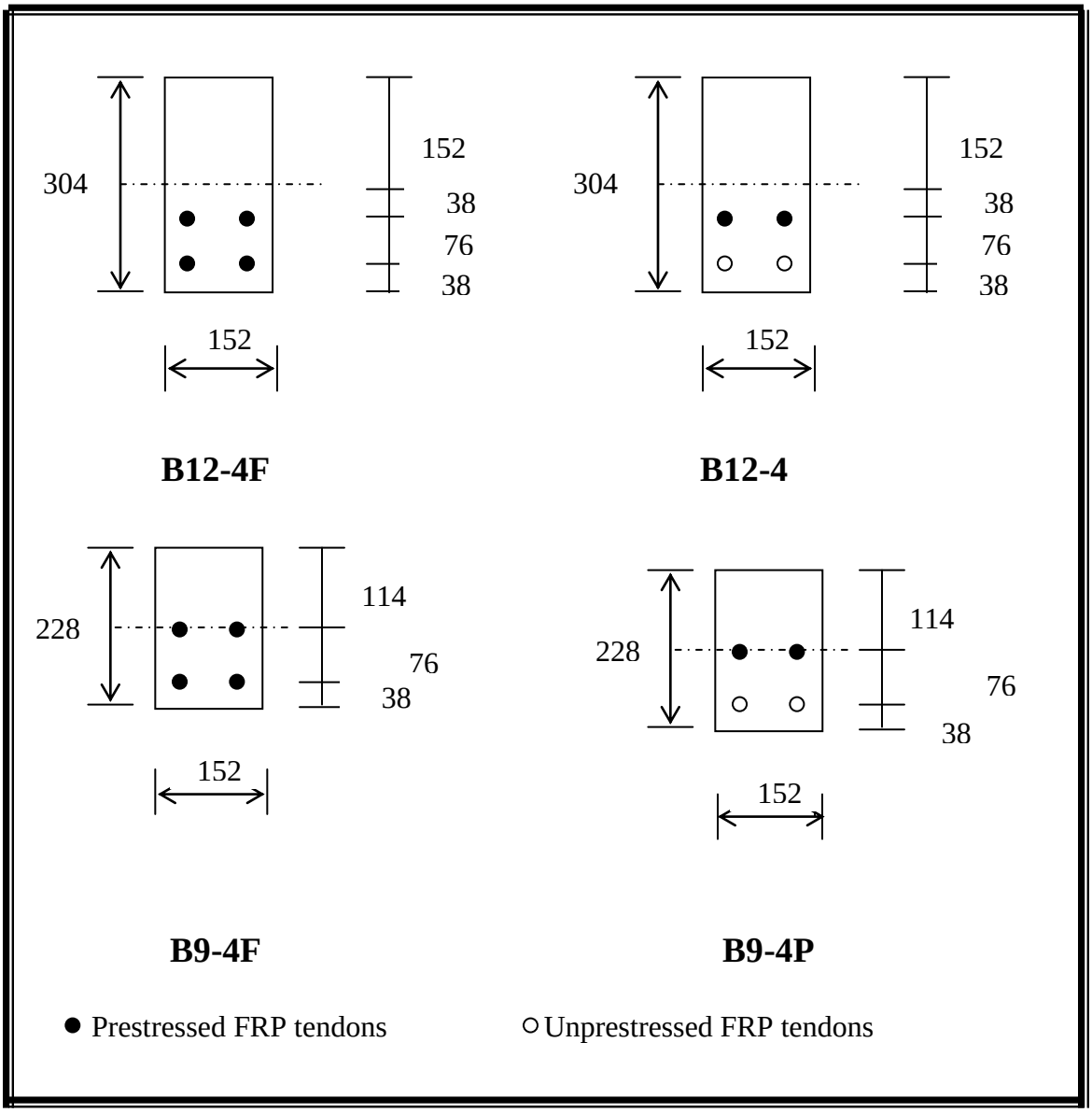

Fig. (11): Sections in tested beams.

Tikrit Journal of Eng. Sciences/Vol.15/No.1/March 2008, (30-51)

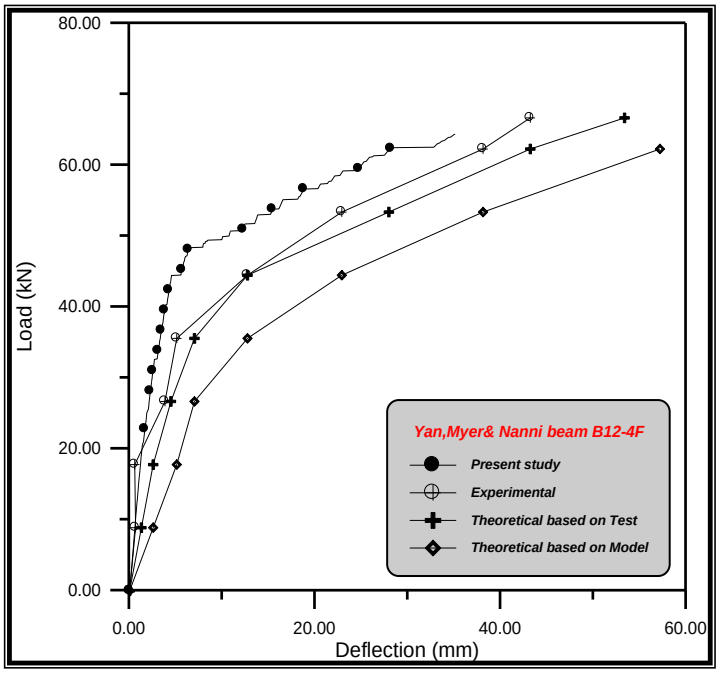

Fig.(13) Load-deflection curve of Yan et al. beam B12-4F (6)

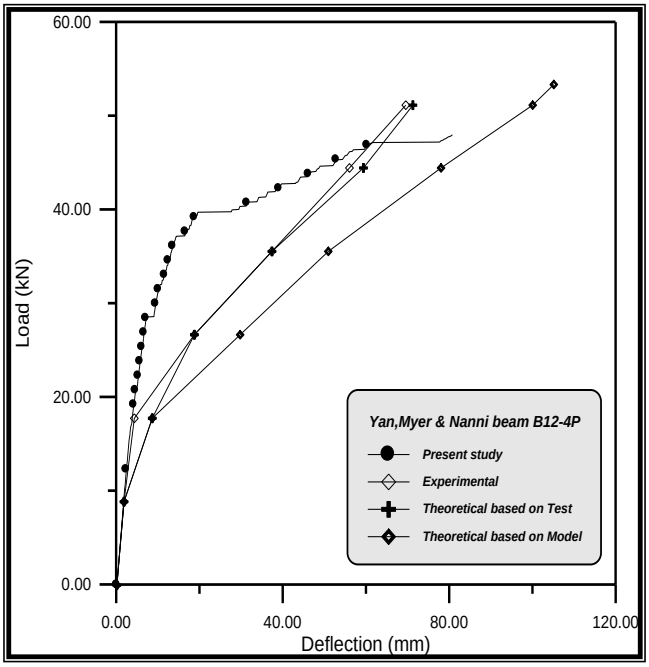

Fig.(15): Distribution of strains over mid-span section of beam B12-4F

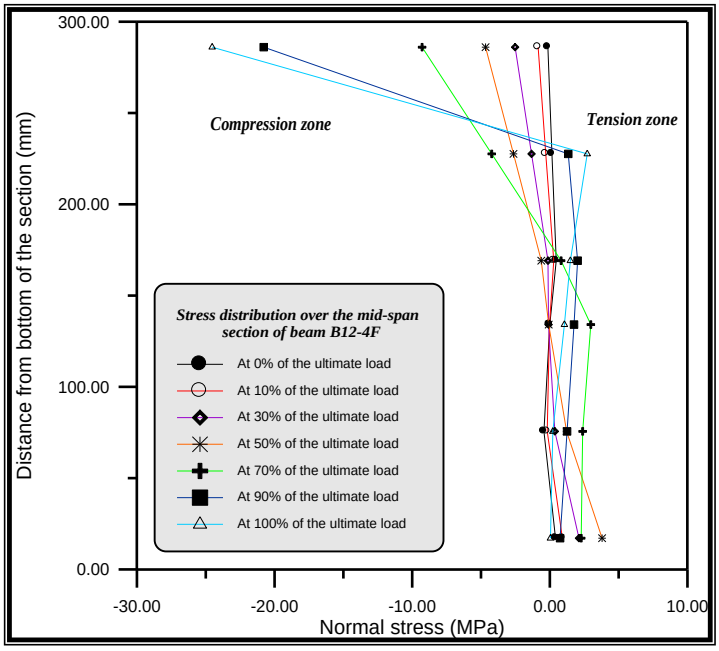

Fig.(14) Distribution of normal stress over mid-span section of beam B12-4F

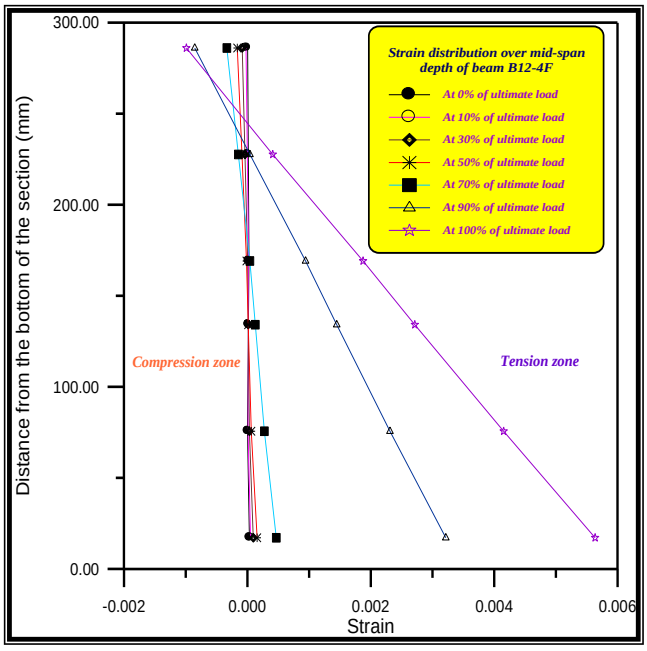

Fig.(16): Load-deflection curve of beam B12-4P

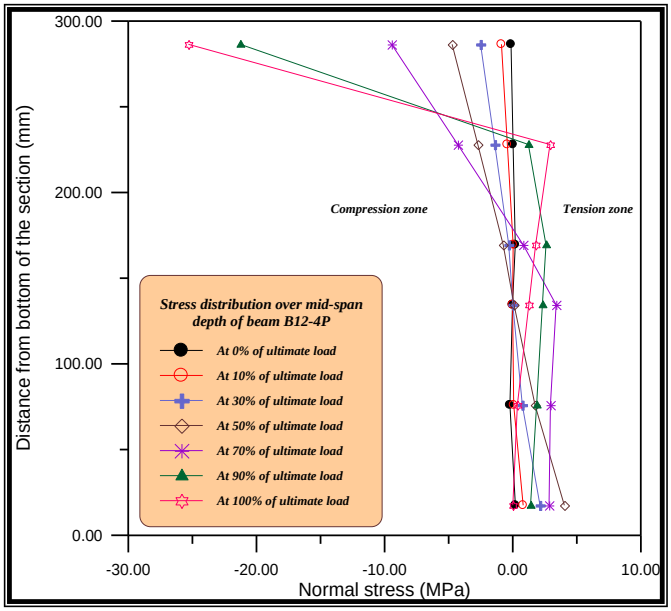

Fig.(17)Distribution of stresses along mid-span depth of beam B12-4P

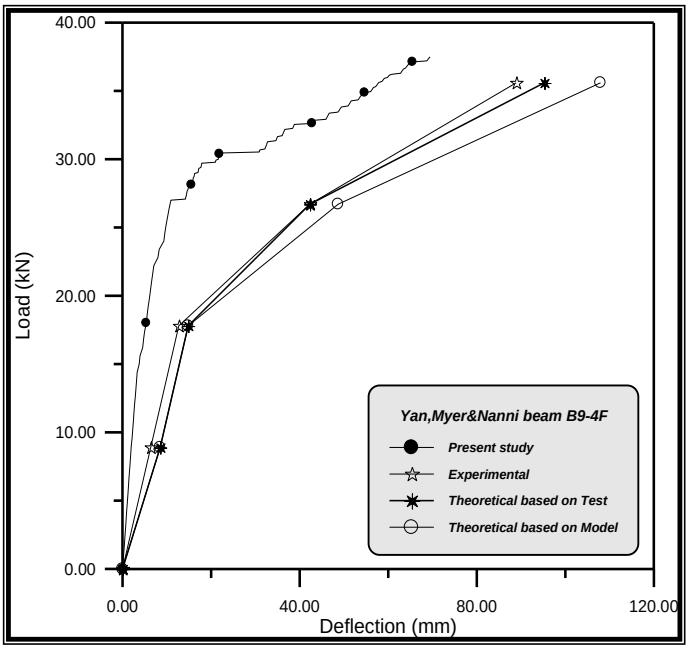

Fig.(19): Load-deflection curve of beam B9-4F

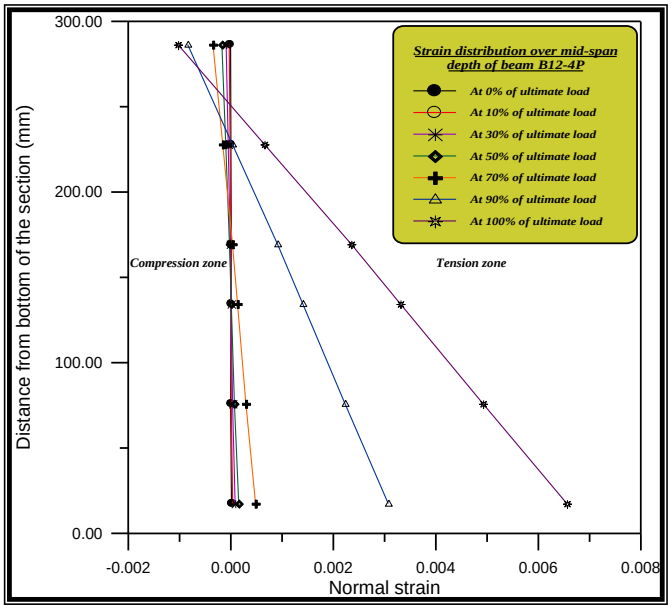

Fig.(18):Strain distribution along mid-span depth of beam B12-4P

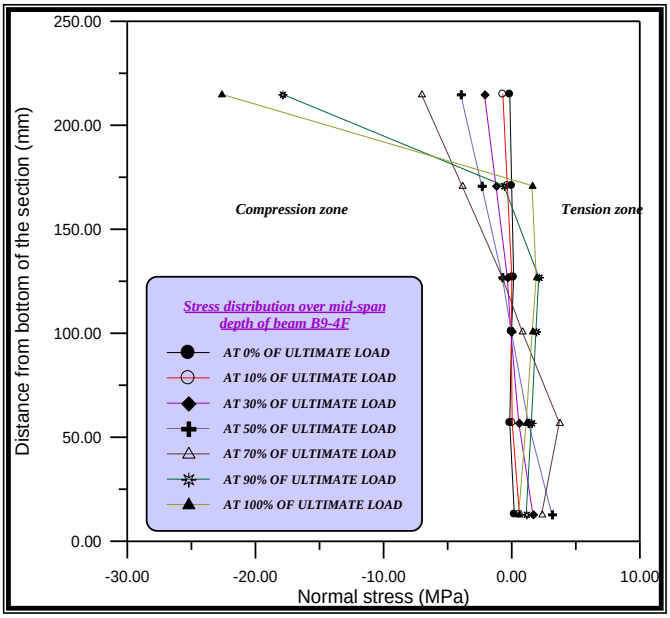

Fig.(20): Stress distribution along mid-span depth of beam B9-4F

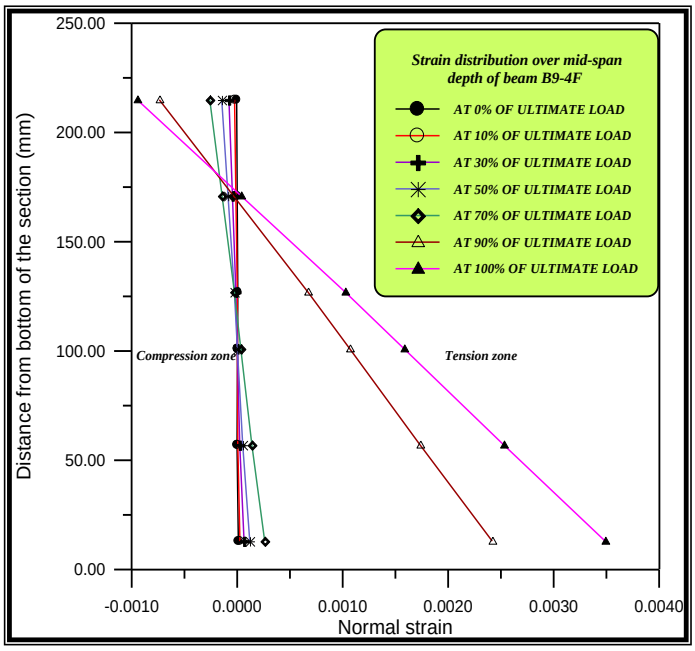

Fig.(21) Strain distribution along mid-span depth of beam B9-4F

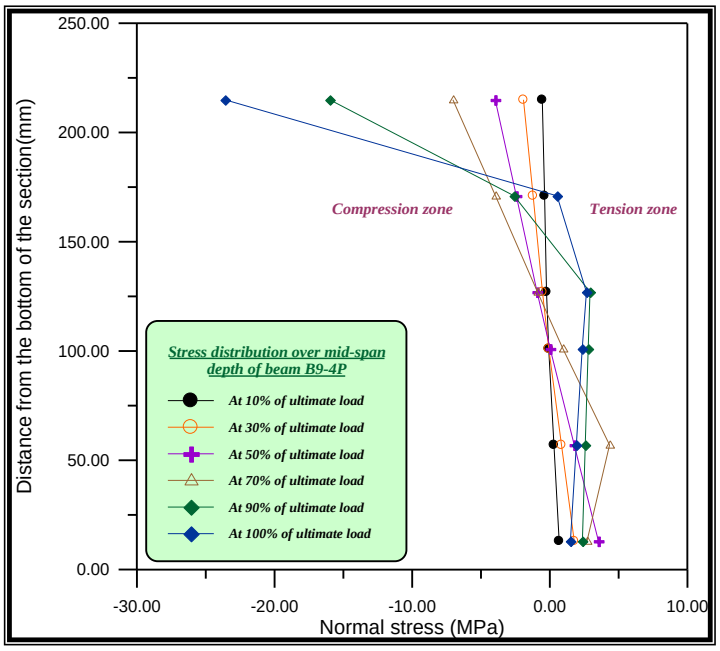

Fig.(23) Stress distribution on mid-span depth of beam B9-4P

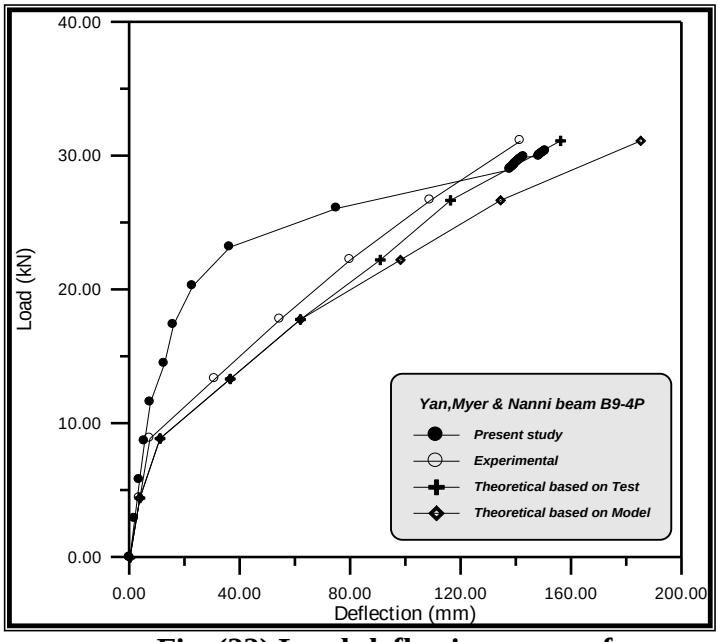

Fig. (22) Load-deflection curve of beam B9-4P

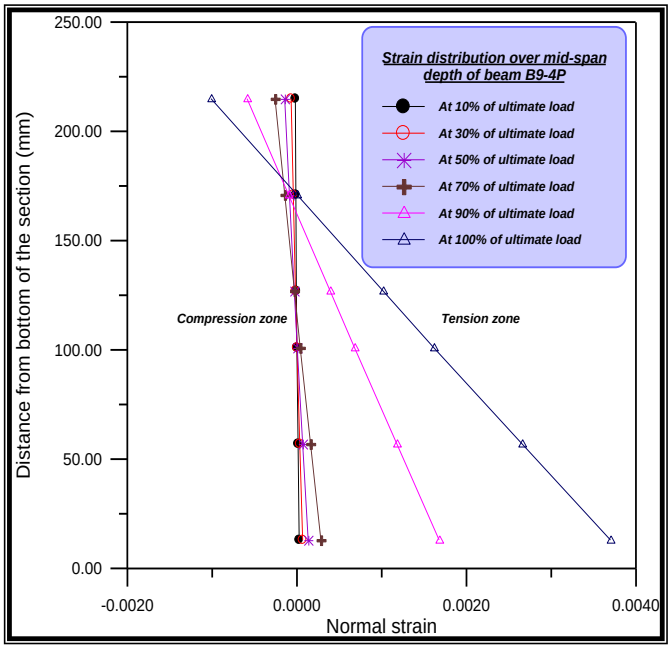

Fig.(24) Strain distribution along mid-span depth of beam B9-4P

التحليل اللاخطي للعتبات المسبقة الجهد المسلحة بحبال CFRP والمعرضة الى حمل ساكن متزايد

د. حسين محمد حسين
استاذ
قسم الهندسة المدنية
الجامعة المستنصرية

د. نزار كامل العقيلي
استاذ مساعد
قسم الهندسة المدنية
جامعة بغداد

د. حاكم سعيد القريشي
استاذ مساعد
المعهد التقني
النجف

الخلاصة

تم بهذا العمل تطوير برنامج لأجراء التحليل اللاخطي (لاخطية المادة) لعتبات خرسانية مسبقة الجهد باستعمال حبال كاربونية مسلحة بألياف بوليمرية (CFRP) عوضا عن حديد التسليح الاعتيادي.تتضمن صفات هذه المادة مقاومتها العالية، خفتها، وعدم تأثرها بالصدأ والحيز المغناطيسي.لا تزال هذه المادة تحت الدراسة والتحري ولهذا تحتاج الى عمل متواصل كي تكون نافعة في تصميم الخرسانة. تم استعمال أربعة عتبات فحصت من قبل يان وآخرين في برنامج حاسوبي مطور للوصول إلى مدخل تحليلي معين لتصميم وتحليل هكذا عتبات لعدم وجود تحديدات أو توصيات تغطي هذه المادة في المدونات. يستخدم البرنامج التحليل بالعناصر المحددة من خلال تقسيم العتبات إلى عناصر طابوقية متساوية العوامل ذات عشرين عقدة. أن النتائج التي تم الحصول عليها جيدة بالمقارنة مع النتائج العملية.